

## Search for Invisible Decays of the $J/\psi$ in $\psi(2S) \rightarrow \pi^+\pi^-J/\psi$

M. Ablikim<sup>1</sup>, J. Z. Bai<sup>1</sup>, Y. Ban<sup>12</sup>, X. Cai<sup>1</sup>, H. F. Chen<sup>17</sup>, H. S. Chen<sup>1</sup>, H. X. Chen<sup>1</sup>, J. C. Chen<sup>1</sup>, Jin Chen<sup>1</sup>, Y. B. Chen<sup>1</sup>, Y. P. Chu<sup>1</sup>, Y. S. Dai<sup>19</sup>, L. Y. Diao<sup>9</sup>, Z. Y. Deng<sup>1</sup>, Q. F. Dong<sup>15</sup>, S. X. Du<sup>1</sup>, J. Fang<sup>1</sup>, S. S. Fang<sup>1a</sup>, C. D. Fu<sup>15</sup>, C. S. Gao<sup>1</sup>, Y. N. Gao<sup>15</sup>, S. D. Gu<sup>1</sup>, Y. T. Gu<sup>4</sup>, Y. N. Guo<sup>1</sup>, Z. J. Guo<sup>16b</sup>, F. A. Harris<sup>16</sup>, K. L. He<sup>1</sup>, M. He<sup>13</sup>, Y. K. Heng<sup>1</sup>, J. Hou<sup>11</sup>, H. M. Hu<sup>1</sup>, J. H. Hu<sup>3</sup>, T. Hu<sup>1</sup>, X. T. Huang<sup>13</sup>, X. B. Ji<sup>1</sup>, X. S. Jiang<sup>1</sup>, X. Y. Jiang<sup>5</sup>, J. B. Jiao<sup>13</sup>, D. P. Jin<sup>1</sup>, S. Jin<sup>1</sup>, Y. F. Lai<sup>1</sup>, G. Li<sup>1c</sup>, H. B. Li<sup>1</sup>, J. Li<sup>1</sup>, R. Y. Li<sup>1</sup>, S. M. Li<sup>1</sup>, W. D. Li<sup>1</sup>, W. G. Li<sup>1</sup>, X. L. Li<sup>1</sup>, X. N. Li<sup>1</sup>, X. Q. Li<sup>11</sup>, Y. F. Liang<sup>14</sup>, H. B. Liao<sup>1</sup>, B. J. Liu<sup>1</sup>, C. X. Liu<sup>1</sup>, F. Liu<sup>6</sup>, Fang Liu<sup>1</sup>, H. H. Liu<sup>1</sup>, H. M. Liu<sup>1</sup>, J. Liu<sup>12d</sup>, J. B. Liu<sup>1</sup>, J. P. Liu<sup>18</sup>, Jian Liu<sup>1</sup>, Q. Liu<sup>16</sup>, R. G. Liu<sup>1</sup>, Z. A. Liu<sup>1</sup>, Y. C. Lou<sup>5</sup>, F. Lu<sup>1</sup>, G. R. Lu<sup>5</sup>, J. G. Lu<sup>1</sup>, C. L. Luo<sup>10</sup>, F. C. Ma<sup>9</sup>, H. L. Ma<sup>2</sup>, L. L. Ma<sup>1e</sup>, Q. M. Ma<sup>1</sup>, Z. P. Mao<sup>1</sup>, X. H. Mo<sup>1</sup>, J. Nie<sup>1</sup>, S. L. Olsen<sup>16</sup>, R. G. Ping<sup>1</sup>, N. D. Qi<sup>1</sup>, H. Qin<sup>1</sup>, J. F. Qiu<sup>1</sup>, Z. Y. Ren<sup>1</sup>, G. Rong<sup>1</sup>, X. D. Ruan<sup>4</sup>, L. Y. Shan<sup>1</sup>, L. Shang<sup>1</sup>, C. P. Shen<sup>16</sup>, D. L. Shen<sup>1</sup>, X. Y. Shen<sup>1</sup>, H. Y. Sheng<sup>1</sup>, H. S. Sun<sup>1</sup>, S. S. Sun<sup>1</sup>, Y. Z. Sun<sup>1</sup>, Z. J. Sun<sup>1</sup>, X. Tang<sup>1</sup>, G. L. Tong<sup>1</sup>, G. S. Varner<sup>16</sup>, D. Y. Wang<sup>1f</sup>, L. Wang<sup>1</sup>, L. L. Wang<sup>1</sup>, L. S. Wang<sup>1</sup>, M. Wang<sup>1</sup>, P. Wang<sup>1</sup>, P. L. Wang<sup>1</sup>, Y. F. Wang<sup>1</sup>, Z. Wang<sup>1</sup>, Z. Y. Wang<sup>1</sup>, Zheng Wang<sup>1</sup>, C. L. Wei<sup>1</sup>, D. H. Wei<sup>1</sup>, U. Wiedner<sup>20</sup>, Y. Weng<sup>1</sup>, N. Wu<sup>1</sup>, X. M. Xia<sup>1</sup>, X. X. Xie<sup>1</sup>, G. F. Xu<sup>1</sup>, X. P. Xu<sup>6</sup>, Y. Xu<sup>11</sup>, M. L. Yan<sup>17</sup>, H. X. Yang<sup>1</sup>, Y. X. Yang<sup>3</sup>, M. H. Ye<sup>2</sup>, Y. X. Ye<sup>17</sup>, G. W. Yu<sup>1</sup>, C. Z. Yuan<sup>1</sup>, Y. Yuan<sup>1</sup>, S. L. Zang<sup>1</sup>, Y. Zeng<sup>7</sup>, B. X. Zhang<sup>1</sup>, B. Y. Zhang<sup>1</sup>, C. C. Zhang<sup>1</sup>, D. H. Zhang<sup>1</sup>, H. Q. Zhang<sup>1</sup>, H. Y. Zhang<sup>1</sup>, J. W. Zhang<sup>1</sup>, J. Y. Zhang<sup>1</sup>, S. H. Zhang<sup>1</sup>, X. Y. Zhang<sup>13</sup>, Yiyun Zhang<sup>14</sup>, Z. X. Zhang<sup>12</sup>, Z. P. Zhang<sup>17</sup>, D. X. Zhao<sup>1</sup>, J. W. Zhao<sup>1</sup>, M. G. Zhao<sup>1</sup>, P. P. Zhao<sup>1</sup>, W. R. Zhao<sup>1</sup>, Z. G. Zhao<sup>1g</sup>, H. Q. Zheng<sup>12</sup>, J. P. Zheng<sup>1</sup>, Z. P. Zheng<sup>1</sup>, L. Zhou<sup>1</sup>, K. J. Zhu<sup>1</sup>, Q. M. Zhu<sup>1</sup>, Y. C. Zhu<sup>1</sup>, Y. S. Zhu<sup>1</sup>, Z. A. Zhu<sup>1</sup>, B. A. Zhuang<sup>1</sup>, X. A. Zhuang<sup>1</sup>, B. S. Zou<sup>1</sup>

(BES Collaboration)

<sup>1</sup> *Institute of High Energy Physics, Beijing 100049, People's Republic of China*

<sup>2</sup> *China Center for Advanced Science and Technology(CCAST), Beijing 100080, People's Republic of China*

<sup>3</sup> *Guangxi Normal University, Guilin 541004, People's Republic of China*

<sup>4</sup> *Guangxi University, Nanning 530004, People's Republic of China*

<sup>5</sup> *Henan Normal University, Xinxiang 453002, People's Republic of China*

<sup>6</sup> *Huazhong Normal University, Wuhan 430079, People's Republic of China*

<sup>7</sup> *Hunan University, Changsha 410082, People's Republic of China*

<sup>8</sup> *Jinan University, Jinan 250022, People's Republic of China*

<sup>9</sup> *Liaoning University, Shenyang 110036, People's Republic of China*

<sup>10</sup> *Nanjing Normal University, Nanjing 210097, People's Republic of China*

<sup>11</sup> *Nankai University, Tianjin 300071, People's Republic of China*

<sup>12</sup> *Peking University, Beijing 100871, People's Republic of China*

<sup>13</sup> *Shandong University, Jinan 250100, People's Republic of China*

<sup>14</sup> *Sichuan University, Chengdu 610064, People's Republic of China*

<sup>15</sup> *Tsinghua University, Beijing 100084, People's Republic of China*

<sup>16</sup> *University of Hawaii, Honolulu, HI 96822, USA*

<sup>17</sup> *University of Science and Technology of China, Hefei 230026, People's Republic of China*

<sup>18</sup> *Wuhan University, Wuhan 430072, People's Republic of China*

<sup>19</sup> *Zhejiang University, Hangzhou 310028, People's Republic of China*

<sup>20</sup> *Institut für Experimentalphysik I, Ruhr-University Bochum, D-44780 Bochum, Germany*

<sup>a</sup> *Current address: DESY, D-22607, Hamburg, Germany*

<sup>b</sup> *Current address: Johns Hopkins University, Baltimore, MD 21218, USA*

<sup>c</sup> *Current address: Universite Paris XI, LAL-Bat. 208- -BP34, 91898- ORSAY Cedex, France*

<sup>d</sup> *Current address: Max-Planck-Institut fuer Physik, Foehringer Ring 6, 80805 Munich, Germany*

<sup>e</sup> *Current address: University of Toronto, Toronto M5S 1A7, Canada*

<sup>f</sup> *Current address: CERN, CH-1211 Geneva 23, Switzerland*

<sup>g</sup> *Current address: University of Michigan, Ann Arbor, MI 48109, USA*

(Dated: October 29, 2018)

Using  $\psi(2S) \rightarrow \pi^+\pi^-J/\psi$  events in a sample of 14.0 million  $\psi(2S)$  decays collected with the BES-II detector, a search for the decay of the  $J/\psi$  to invisible final states is performed. The  $J/\psi$  peak in the distribution of masses recoiling against the  $\pi^+\pi^-$  is used to tag  $J/\psi$  invisible decays. No signal is found, and an upper limit at the 90% confidence level is determined to be  $1.2 \times 10^{-2}$

for the ratio  $\frac{\mathcal{B}(J/\psi \rightarrow \text{invisible})}{\mathcal{B}(J/\psi \rightarrow \mu^+ \mu^-)}$ . This is the first search for  $J/\psi$  decays to invisible final states.

PACS numbers: 13.25.Gv, 95.30.Cq

Invisible decays of quarkonium states such as  $J/\psi$  and  $\Upsilon$ , etc., offer a window into what may lie beyond the standard model (SM) [1, 2, 3]. This is because, aside from neutrinos, the SM includes no other invisible particles that these states can decay into. In the SM, the predicted branching fraction for  $J/\psi \rightarrow \nu\bar{\nu}$  is

$$\mathcal{B}(J/\psi \rightarrow \nu\bar{\nu}) = 4.54 \times 10^{-7} \times \mathcal{B}(J/\psi \rightarrow e^+ e^-) \quad (1)$$

with a small uncertainty (2-3%) [1, 4]. However, new physics beyond the SM might enhance the branching fraction of  $J/\psi$  invisible decays. One possibility is the decay into light dark matter (LDM) particles mediated by a new, electrically neutral spin-1 gauge boson  $U$ , which could significantly increase the invisible decay rate [5]. On the other hand,  $C$ -even operators  $\bar{q}q$  or  $\bar{q}\gamma_5 q$  do not contribute to invisible decays of the  $J/\psi$  [2, 3]. Thus, there would be no contributions from a possible scalar or pseudoscalar exchange to the decay of  $J/\psi$  [3, 6].

Astronomical observations of a bright 511 keV  $\gamma$ -ray line from the galactic bulge have been reported by the SPI spectrometer on the International Gamma-Ray Astrophysics Lab (INTEGRAL) satellite [7]. The corresponding galactic positron flux, as well as the smooth symmetric morphology of the 511 keV emission, may be interpreted as originating from the annihilation of LDM particles into  $e^+e^-$  pairs [5]. It is of interest to search for such light invisible particles in collider experiments. CLEO reported an upper bound on  $\Upsilon(1S) \rightarrow \gamma + \text{invisible}$ , which is sensitive to dark matter candidates lighter than about 3 GeV/ $c^2$  and also provides an upper limit on the axial coupling of a new  $U$  boson to the  $b$  quark [8]. Recently, both CLEO and Belle reported upper limits on  $\Upsilon(1S) \rightarrow \text{invisible}$  decays [9]. The first experimental limits on invisible decays of the  $\eta$  and  $\eta'$  mesons have been reported by the BES Collaboration [10]; these can be used to constrain the mass of the LDM particles and couplings of new bosons to light quarks. Here, we present the first search for  $J/\psi$  decays to invisible final states.

BES-II is the upgraded version of the BES-I detector [11]. A 12-layer vertex chamber (VC) surrounding the beam pipe provides trigger and position information. This detector efficiently detects the presence of charged tracks over 97% of the total solid angle. A forty-layer main drift chamber (MDC), located radially outside the VC, provides trajectory and energy loss ( $dE/dx$ ) information for charged tracks over 85% of the total solid angle. The momentum resolution is  $\sigma_p/p = 0.017\sqrt{1+p^2}$  ( $p$  in GeV/ $c$ ), and the  $dE/dx$  resolution for hadron tracks is  $\sim 8\%$ . An array of 48 scintillation counters surrounding the MDC measures the time-of-flight (TOF) of charged tracks with a resolution of  $\sim 200$  ps for hadrons. Outside of the TOF counters is a 12-radiation-length barrel shower counter

(BSC) composed of gas tubes interleaved with lead sheets. This measures the energies of electrons and photons over  $\sim 80\%$  of the total solid angle with an energy resolution of  $\sigma_E/E = 22\%/\sqrt{E}$  ( $E$  in GeV). Outside of the solenoidal coil, which provides a 0.4 Tesla magnetic field over the tracking volume, is an iron flux return that is instrumented with three double layers of counters that identify muons of momenta greater than 0.5 GeV/ $c$ .

In order to detect invisible  $J/\psi$  decays, we use  $\psi(2S) \rightarrow \pi^+\pi^- J/\psi$  and infer the presence of the  $J/\psi$  from the  $J/\psi$  peak in the distribution of mass recoiling against the  $\pi^+\pi^-$ . In this analysis, we use a 19.72 pb $^{-1}$  data sample collected at the peak of the  $\psi(2S)$  resonance and a 6.42 pb $^{-1}$  data sample collected off-resonance at a center-of-mass energy of  $\sqrt{s} = 3.65$  GeV. The data were recorded in the BES-II detector operating at the Beijing Electron Positron Collider (BEPC). The data sample contains 14.0 million  $\psi(2S)$  decays.

In the search for  $J/\psi$  invisible decays, invisible means nothing besides the two pions is seen in either the tracking or calorimetry systems of the detector. The charged-track trigger in BES-II requires at least one hit in the 48 barrel TOF counter array, one track in the VC and MDC, and at least 100 MeV of energy deposit in the BSC [11, 12]. This trigger is sensitive to two soft pions from the  $\psi(2S)$  decay of the signal events.

Events with only two charged tracks with zero net charge are selected. Each charged track is required to be well fitted by a helix and to have a polar angle,  $\theta$ , within the fiducial region  $|\cos\theta| < 0.8$ . To ensure that the tracks originate from the interaction region, we require  $V_{xy} = \sqrt{V_x^2 + V_y^2} < 2$  cm and  $|V_z| < 20$  cm, where  $V_x$ ,  $V_y$ , and  $V_z$  are the  $x$ ,  $y$ , and  $z$  coordinates of the point of closest approach of each charged track to the beam axis. In addition, the momentum of each charged track must be less than 0.4 GeV/ $c$ . Particle identification (PID) is performed with the combined TOF and  $dE/dx$  information, and both charged tracks must be identified as pions. The invariant mass of the  $\pi^+\pi^-$  pair is required to be larger than 0.35 GeV/ $c^2$ .

In BES-II, high momentum charged tracks with  $|\cos\theta| < 0.8$  traverse the full radial extent of the MDC are detected and reconstructed efficiently. Tracks with lower momentum and/or at larger angles miss some or all of the MDC layers and may not be reliably reconstructed. However, tracks that originate from the center of the interaction point with a polar angle in the range  $|\cos\theta| < 0.97$  penetrate at least six layers of the inner vertex chamber; Although these tracks are not fully reconstructed, their presence can be inferred with high efficiency from track segments reconstructed from three or more VC hits. Events with indications

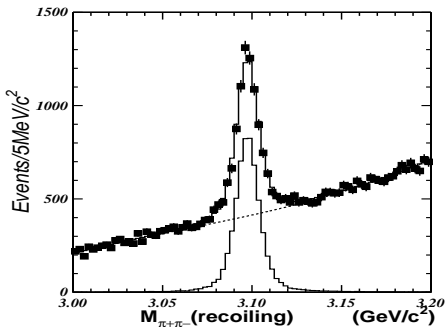


FIG. 1: Distribution of masses recoiling against the  $\pi^+\pi^-$  for  $\psi(2S) \rightarrow \pi^+\pi^- J/\psi, J/\psi \rightarrow \text{invisible}$  candidate events. Dots with error bars denote data. The lower histogram is the signal shape from  $\psi(2S) \rightarrow \pi^+\pi^- J/\psi, J/\psi \rightarrow \mu^+\mu^-$  events. The upper histogram and the dashed curve are from the fit.

of additional charged tracks anywhere in the region of angular coverage of the vertex chamber are rejected.

Each reconstructed BSC cluster is required to have an energy greater than 10 MeV and to have a cluster profile consistent with that of a shower in the BSC. The number of unassociated neutral clusters, which do not match with either charged track in the MDC, is required to be zero in order to suppress backgrounds from  $J/\psi$  decaying into neutral final states.

Figure 1 shows the distribution of masses recoiling against the  $\pi^+\pi^-$  pair for candidate events. A clear  $J/\psi$  peak is evident for the data taken at the  $\psi(2S)$ , while the smooth background under the  $J/\psi$  peak from the QED contribution is consistent with the distribution obtained with off-resonance data at  $\sqrt{s} = 3.65$  GeV after normalizing to the luminosity at  $\sqrt{s} = M_{\psi(2S)}$ .

By measuring the ratio of invisible  $J/\psi$  decays to  $J/\psi \rightarrow \mu^+\mu^-$ , many uncertainties cancel, including those related to the number of  $J/\psi$  decays, the soft pion tracking efficiencies, and the zero neutral cluster requirement. First, two soft pions are chosen with the same selection criteria as used for  $\psi(2S) \rightarrow \pi^+\pi^- J/\psi, J/\psi \rightarrow \text{invisible}$ . Then, we require that there are two muons in addition to the two soft pions. Two selection criteria are used to identify muons. One is that the momentum of each track is larger than 0.7 GeV/c. The other is that  $R$ , which is defined as

$$R = \sqrt{\left(\frac{E_{sc1}}{p_1} - 1\right)^2 + \left(\frac{E_{sc2}}{p_2} - 1\right)^2},$$

be larger than 1.0 in order to reject  $J/\psi \rightarrow e^+e^-$  events. Here,  $E_{sc1}$  and  $E_{sc2}$  denote the deposited energies in the BSC, and  $p_1$  and  $p_2$  denote their momenta. Figure 2 (a) shows the  $R$  distributions for data and Monte Carlo (MC) simulated events. For

each event, the total energy of the four charged tracks,  $E_{tot}$ , is required to be larger than 3.6 GeV, as shown in Fig. 2 (b). The small difference between the  $E_{tot}$  distributions for data and MC simulation is caused by imperfect simulation of soft pions, an effect that is considered in the systematic error study. The requirement on the number of unassociated neutral clusters or extra charged tracks is the same as that for  $\psi(2S) \rightarrow \pi^+\pi^- J/\psi, J/\psi \rightarrow \text{invisible}$  so that the systematic uncertainties cancel in the ratio. Figure 3 shows the  $M_{\pi^+\pi^-}^{\text{recoil}}$  distribution for  $\pi^+\pi^-\mu^+\mu^-$  final states for data and MC simulation after the above selection. Compared to the data distribution, the MC sample has a shift of 1.0 MeV/c<sup>2</sup>, which is also caused by the imperfect simulation of soft pions. The number of  $\psi(2S) \rightarrow \pi^+\pi^- J/\psi, J/\psi \rightarrow \mu^+\mu^-$  events selected is  $43429 \pm 208$  where the error is statistical, and the corresponding MC-determined detection efficiency is 14.5%.

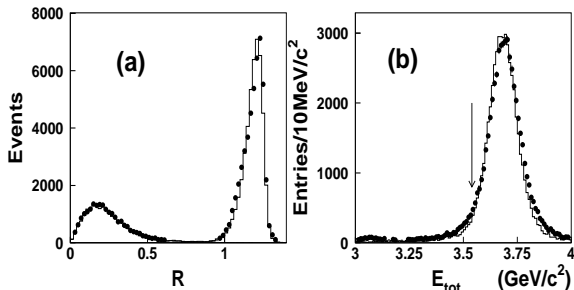


FIG. 2: (a) Distributions of  $R$  for the two non-pion tracks in  $\psi(2S) \rightarrow \pi^+\pi^- J/\psi, J/\psi \rightarrow \ell^+\ell^-$ . (b) Distributions of  $E_{tot}$  for  $\psi(2S) \rightarrow \pi^+\pi^- J/\psi, J/\psi \rightarrow \mu^+\mu^-$ . The histogram denotes MC and dots with error bars denote data.

Exclusive channels that are potential backgrounds are studied using full MC simulations in order to determine their contamination. The sources of the backgrounds can be divided into two classes. Class I is

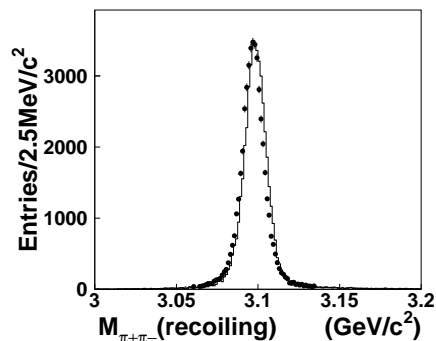


FIG. 3: Distribution of mass recoiling against the  $\pi^+\pi^-$  pair for  $\psi(2S) \rightarrow \pi^+\pi^-\mu^+\mu^-$  candidate events. The histogram denotes MC simulation and dots with errors denote data.

mainly from final states without a  $J/\psi$ , such as the continuum processes  $e^+e^- \rightarrow q\bar{q}$  and  $\tau^+\tau^-$  ( $q = u, d$  and  $s$  quarks). The smooth backgrounds under the  $J/\psi$  peak in Fig. 1 are from "Class I". Class II is from  $\psi(2S) \rightarrow \pi^+\pi^- J/\psi$ , where the  $J/\psi$  decays into other modes than the true invisible final state. For this case, the  $J/\psi$  decay products are either outside of the detector acceptance, or are inside but are undetected. For these kinds of backgrounds, there is a  $J/\psi$  peak in the  $M_{\pi^+\pi^-}^{\text{recoil}}$  distribution that is identical to the invisible signal. The largest sources of "peaking backgrounds" are from the  $J/\psi$  decays to  $\ell^+\ell^-$  ( $\ell = e, \mu$ ), where the two tracks tend to be back to back, so when one track escapes into the forward insensitive region, the other track tends to escape into the backward insensitive region. This is a geometric effect and its size is determined from Monte Carlo simulation. Other sources of backgrounds are from decays to  $n\bar{n}$ , where the neutron and anti-neutron leave no hit information in the detector. An additional potential background comes from  $J/\psi$  decays to  $n\bar{n}\pi^0$ , in which neither of the two photons from  $\pi^0$  decay are within the detector acceptance and the neutron and antineutron either have no hit information in the detector or miss the sensitive region of the detector.

The systematic uncertainties on the number of expected background events caused by the selection criteria are estimated using special event samples. For the dominant backgrounds from  $J/\psi$  decays to  $\ell^+\ell^-$ , the uncertainty is mainly from the difference between data and MC simulation of the contamination from two missing leptons. We determine this systematic error using  $J/\psi \rightarrow K_S K^\pm \pi^\mp$ , in which only the  $K_S$  and the charged pion are required in event selection. This provides a large sample of ( $\simeq 38.6\text{K}$ ) tagged charged kaons in the detector. With these, we measure the probability for a charged kaon to be "invisible," *i.e.*, to evade the extra track requirements, to be  $(3.49 \pm 0.09)\%$ . A MC simulation of this process gives an invisibility probability of  $(3.13 \pm 0.07)\%$ . The difference of  $\simeq 10\%$  between the measured and simulated probabilities is taken as a systematic error for peaking backgrounds from  $J/\psi$  decays to  $\ell^+\ell^-$  and  $p\bar{p}$ .

In estimating the expected background contamination from  $J/\psi \rightarrow n\bar{n}$ , we assume the branching fraction and its corresponding uncertainty for  $J/\psi \rightarrow n\bar{n}$  are the same as those for  $J/\psi \rightarrow p\bar{p}$  as is expected according to SU(2) symmetry. Similarly, since the measurements of branching fraction for  $J/\psi \rightarrow n\bar{n}\pi^0$  is not currently available, we assume the branching fraction and its corresponding uncertainty for  $J/\psi \rightarrow n\bar{n}\pi^0$  are the same as those for  $J/\psi \rightarrow p\bar{p}\pi^0$ . For the  $J/\psi \rightarrow n\bar{n}$  background, the main uncertainty is from the difference between data and MC simulation in the  $n\bar{n}$  rejection rate based on the requirement of zero clusters in the BSC. The distribution of the number of clusters associated with  $n\bar{n}$  is obtained from two control samples,  $J/\psi \rightarrow p\bar{n}\pi^- + c.c.$  and  $J/\psi \rightarrow \pi^+\pi^- p\bar{p}$ . First, the distribution of the number of clusters ex-

TABLE I: Expected number of events ( $N_{bg}$ ) and efficiencies for peaking backgrounds.

Background channel ( $\psi(2S) \rightarrow \pi^+\pi^- J/\psi, J/\psi \rightarrow$ )	Efficiency (%)	Expected $N_{bg}$
$\mu^+\mu^-$	0.964	$2543 \pm 254$
$e^+e^-$	0.907	$2393 \pm 240$
$n\bar{n}$	10.46	$1011 \pm 85$
$p\bar{p}$	0.434	$42 \pm 13$
$n\bar{n}\pi^0$	0.486	$29 \pm 10$
Total		$6018 \pm 514$

pected for  $p\bar{p}\pi^+\pi^- n\bar{n}$  can be obtained by combining the  $p\bar{n}\pi^-$  and  $\bar{p}n\pi^+$  samples. Second, using the control sample,  $J/\psi \rightarrow \pi^+\pi^- p\bar{p}$ , the cluster distribution for  $n\bar{n}$  can be obtained by subtracting the  $p\bar{p}\pi^+\pi^-$  distribution from the  $p\bar{p}\pi^+\pi^- n\bar{n}$  distribution. The distributions of the number of clusters between data from the control sample and MC simulation are compared, and the difference between MC and data for the number of  $n\bar{n}$  events with zero BSC clusters is a 7.6% effect, which is taken as a systematic error. The estimated contributions from the peaking backgrounds are summarized in Table I. The error on the expected number of events for each peaking background includes the contributions from both the branching fraction uncertainty and the estimated systematic error. For  $J/\psi \rightarrow \ell^+\ell^-$  and  $p\bar{p}$ , the dominant uncertainty arises from the geometrical acceptance and their associated errors are entirely correlated.

A  $\chi^2$  fit is used to extract the number of  $J/\psi$  events in the distribution of mass recoiling against the  $\pi^+\pi^-$  in the range  $3.0 \text{ GeV}/c^2 < M_{\pi^+\pi^-}^{\text{recoil}} < 3.2 \text{ GeV}/c^2$ . Here, the shape used to describe the signal comes from the  $\pi^+\pi^-$  recoil mass spectrum from the  $\psi(2S) \rightarrow \pi^+\pi^- J/\psi, J/\psi \rightarrow \mu^+\mu^-$  control sample, and not from the MC simulation due to differences between the data and MC simulation (see Fig. 3). The Class I background is represented by a second-order polynomial. The fit, with  $\chi^2/ndf = 62.6/75$  and shown in Fig. 1, yields  $6424 \pm 137$  events in the peak, which includes the contributions from both signal and peaking backgrounds, since they have the same probability density functions (PDF) in the fit. After subtracting the expected backgrounds listed in Table I from the fitted yields, we get the number of  $\psi(2S) \rightarrow \pi^+\pi^- J/\psi, J/\psi \rightarrow$  invisible events to be  $406 \pm 532$ .

The estimated uncertainties that do not cancel in the ratio are described here. The systematic uncertainty caused by the tracking efficiency in the MDC for the two muons in the control sample is estimated to be 4% [13]. The systematic error for the requirement on  $E_{tot}$  is 1.7%, and the uncertainty caused by the  $R$  requirement in the selection of the control sample,  $\psi(2S) \rightarrow \pi^+\pi^- J/\psi, J/\psi \rightarrow \mu^+\mu^-$ , is determined to be 1.0% by a comparison with and without the  $R$  requirement. The uncertainty from the background

shape, which is used in the fit to  $M_{\pi^+\pi^-}^{\text{recoil}}$  for Class I, is found to be negligible. The uncertainty associated with bin-size and the range of the fit is 1.3%. In order to investigate the uncertainty caused by the trigger, we check the four trigger channels used in the BES-II experiment. The largest systematic error comes from uncertainties in modeling the energy threshold requirement in the BSC. A conservative estimate, based on MC simulation, is that this corresponds to at most a 1% uncertainty in the detection efficiency. The uncertainty of  $\mathcal{B}(J/\psi \rightarrow \mu^+\mu^-)$  is taken from the PDG [14]. The total uncertainty, which is determined by the sum of all sources in quadrature, is 4.9%. Taking this systematic uncertainty into account, the upper limit for the number of events of  $\psi(2S) \rightarrow \pi^+\pi^- J/\psi, J/\psi \rightarrow \text{invisible}$  is 1285 at the 90% confidence level, or a central value of  $406_{-333}^{+539}$  at the 68.3% confidence level from the Feldman-Cousins frequentist approach [15].

Finally, the upper limit on the ratio of  $\mathcal{B}(J/\psi \rightarrow \text{invisible})$  to  $\mathcal{B}(J/\psi \rightarrow \mu^+\mu^-)$  is determined from the relation

$$\begin{aligned} \frac{\mathcal{B}(J/\psi \rightarrow \text{invisible})}{\mathcal{B}(J/\psi \rightarrow \mu^+\mu^-)} &< \frac{N_{UL}^{J/\psi}/\epsilon_{\text{invisible}}}{N_{\mu^+\mu^-}^{J/\psi}/\epsilon_{\mu^+\mu^-}^{J/\psi}} \\ &= 1.2 \times 10^{-2}, \end{aligned} \quad (2)$$

where  $N_{UL}^{J/\psi}$  (1285) is the 90% confidence-level upper limit on the number of  $\psi(2S) \rightarrow \pi^+\pi^- J/\psi, J/\psi \rightarrow \text{invisible}$  events,  $\epsilon_{\text{invisible}}$  (36.8%) is the MC-determined signal efficiency,  $N_{\mu^+\mu^-}^{J/\psi}$  ( $43429 \pm 208$ ) is the number of events for  $\psi(2S) \rightarrow \pi^+\pi^- J/\psi, J/\psi \rightarrow \mu^+\mu^-$  and  $\epsilon_{\mu^+\mu^-}^{J/\psi}$  (14.5%) is the detection efficiency for that decay mode. In addition, the two-sided interval of the number of the measured events for invisible decays,  $N_{\text{invisible}}^{J/\psi}$ , is (73, 945) at the 68.3% confidence

level. The corresponding two-sided interval of the ratio  $\frac{\mathcal{B}(J/\psi \rightarrow \text{invisible})}{\mathcal{B}(J/\psi \rightarrow \mu^+\mu^-)}$  is  $(0.66 \times 10^{-3}, 8.6 \times 10^{-3})$ .

In summary, we performed the first search for invisible decays of the  $J/\psi$  using  $\psi(2S) \rightarrow \pi^+\pi^- J/\psi$  events detected in a sample of 14.0 million  $\psi(2S)$  decays. The upper limit on the ratio  $\frac{\mathcal{B}(J/\psi \rightarrow \text{invisible})}{\mathcal{B}(J/\psi \rightarrow \mu^+\mu^-)}$  at the 90% confidence level is  $1.2 \times 10^{-2}$ . This measurement improves by a factor of 3.5 the bound on the product of the coupling of the  $U$  boson to the  $c$  quark and LDM particles as described in Eqs. (25) and (26) of Ref. [2]. One now has, for a Majorana LDM particle  $\chi$  as in Eq. (26) of Ref. [2], a limit of  $|c_\chi f_{cV}| < 8.5 \times 10^{-3}$ , which is almost a factor of 2 stronger than the corresponding limit  $|c_\chi f_{bV}| < 1.4 \times 10^{-2}$  derived from the invisible decays of the  $\Upsilon(1S)$  as described in Eq. (106) in Ref. [3], where  $c_\chi$  and  $f_{cV}$  ( $f_{bV}$ ) denote the  $U$  boson couplings to the LDM particle  $\chi$  and  $c$  ( $b$ ) quark. We expect a more precise measurement can be obtained in the future BES-III experiment.

The BES collaboration thanks the staff of BEPC and computing center for their hard efforts. We would also thank P. Fayet, R. McElrath and S. H. Zhu for useful discussions and suggestions. This work is supported in part by the National Natural Science Foundation of China under contracts Nos. 10491300, 10225524, 10225525, 10425523, the Chinese Academy of Sciences under contract No. KJ 95T-03, the 100 Talents Program of CAS under Contract Nos. U-11, U-24, U-25, and the Knowledge Innovation Project of CAS under Contract Nos. U-602, U-34 (IHEP), the National Natural Science Foundation of China under Contract No. 10225522 (Tsinghua University), the Swedish research Council (VR), and the Department of Energy under Contract No. DE-FG02-04ER41291 (U Hawaii).

- 
- [1] P. Fayet, Phys. Lett. **B 84**, 421 (1979); P. Fayet, and J. Kaplan, Phys. Lett. **B 269**, 213 (1991); B. McElrath, Phys. Rev. D **72**, 103508 (2005).
- [2] P. Fayet, Phys. Rev. D **74**, 054034 (2006).
- [3] P. Fayet, Phys. Rev. D **75**, 115017 (2007).
- [4] L. N. Chang, O. Lebedev and J. N. Ng, Phys. Lett. **B 441**, 419 (1998).
- [5] C. Boehm and P. Fayet. Nucl. Phys. **B 683**, 219 (2004); C. Boehm and D. Hooper, J. Silk, M. Casse, and J. Paul, Phys. Rev. Lett. **92**, 101301 (2004); P. Fayet. Phys. Rev. D **70**, 023514 (2004); P. Fayet, Phys. Lett. **B 95**, 285 (1980); P. Fayet, Nucl. Phys. **B 187**, 184 (1981); S. H. Zhu, Phys. Rev. D **75**, 115004 (2007).
- [6] J. Ellis, J. F. Gunion, H. E. Haber, L. Roszkowski, and F. Zwirner, Phys. Rev. D **39**, 844 (1989); J. F. Gunion, D. Hooper, and B. McElrath, Phys. Rev. D **73**, 015011 (2006).
- [7] P. Jean *et al.*, Astron. Astrophys. 407, L55 (2003); SPI is the spectrometer aboard INTEGRAL.
- [8] R. Balest, *et al.*, (CLEO Collaboration), Phys. Rev. D **51**, 2053 (1995).
- [9] P. Rubin *et al.*, (CLEO Collaboration), Phys. Rev. D **75**, 031104 (2007); O. Tajima *et al.*, (Belle Collaboration), Phys. Rev. Lett. **98**, 132001 (2007).
- [10] M. Ablikim *et al.*, (BES Collaboration), Phys. Rev. Lett. **97**, 202002 (2006).
- [11] J. Z. Bai *et al.*, (BES Collaboration), Nucl. Instr. Meth. **A 344**, 319 (1994); Nucl. Instr. Meth. **A 458**, 627 (2001).
- [12] J. Z. Bai *et al.*, (BES Collaboration), Phys. Rev. Lett. **84**, 594 (2000).
- [13] M. Ablikim *et al.*, (BES Collaboration), Nucl. Instr. Meth. **A 552**, 344 (2005).
- [14] W. M. Yao *et al.*, Particle Physics Group, J. Phys. G: Nucl. Part. Phys. **33**, 1 (2006).
- [15] G. J. Feldman and R. D. Cousins. Phys. Rev. D **57**, 3873 (1998).